

2 Determinants of high residual post-PCV13 pneumococcal vaccine type carriage in Blantyre, Malawi: a modelling study.

4 Authors

6 J. Lourenço (PhD)^{3,*,#}, U. Obolski(PhD)^{12,13,#}, T.D. Swarthout (MSc)^{1,2,#}, A. Gori (PhD)⁴, N. Bar-
8 Zeev (PhD)^{1,5}, D. Everett (PhD)^{1,6}, A.W. Kamng'ona (PhD)⁷, T.S. Mwalukomo (MMed)⁸, A.A. Mataya (MBBS)¹, C. Mwansambo (MBChB)⁹, M. Banda¹⁰, S. Gupta (PhD)^{3,¥}, N. French (PhD)^{1,11¥},
R.S. Heyderman (PhD)^{1,4,¥}

*Correspondence to: JL, jose.lourenco@zoo.ox.ac.uk

10 # Joint first authors have contributed equally to this manuscript (Lourenço, Obolski, Swarthout)

12 ¥ Joint last authors have contributed equally to this manuscript (Gupta, French, Heyderman)

14

Affiliations

16 1. Malawi-Liverpool-Wellcome Trust Clinical Research Programme, Blantyre, Malawi
2. Clinical Sciences Department, Liverpool School of Tropical Medicine, Liverpool, United Kingdom
18 3. Department of Zoology, University of Oxford, Oxford, United Kingdom
4. Division of Infection & Immunity, University College London, London, United Kingdom
20 5. Department of International Health, Johns Hopkins Bloomberg School of Public Health, Baltimore, USA
6. The Queens Medical Research Institute, University of Edinburgh, Edinburgh
22 7. Department of Biomedical Sciences, College of Medicine, University of Malawi, Blantyre, Malawi
8. Department of Medicine, College of Medicine, University of Malawi, Blantyre, Malawi
24 9. Ministry of Health, Lilongwe, Malawi
10. Ministry of Education, Blantyre, Malawi
26 11. Centre for Global Vaccine Research, Institute of Infection and Global Health, University of Liverpool, United Kingdom
12. School of Public Health, Tel Aviv University, Tel Aviv, Israel
28 13. Porter School of the Environment and Earth Sciences, Tel Aviv University, Tel Aviv, Israel

30 **Keywords:** pneumococcus, pcv13, modelling, malawi, intervention

32

Abbreviations:

34 VT - vaccine type
NVT - non-vaccine type
36 PCV - pneumococcal conjugate vaccine
CI - confidence interval
bMCMC - Bayesian Markov chain Monte Carlo
38 ODE - ordinary-differential equations
FOI - force of infection
40 dVP - duration of vaccine-induced protection

42

Abstract

44

Background: In November 2011, Malawi introduced the 13-valent pneumococcal conjugate vaccine (PCV13) into the routine infant schedule. Four to seven years after introduction (2015-2018), rolling prospective nasopharyngeal carriage surveys were performed in the city of Blantyre. Carriage of *Streptococcus pneumoniae* vaccine serotypes (VT) remained higher than reported in developed countries, and VT impact was surprisingly asymmetric across age-groups. A dynamic transmission model was fit to survey data using a Bayesian Markov-chain Monte Carlo approach, to obtain insights into the determinants of post-PCV13 age-specific VT carriage.

52 **Results:** Accumulation of naturally acquired immunity with age and age-specific transmission potential were both key to reproducing the observed data. VT carriage reduction peaked 54 sequentially over time, earlier in younger and later in older age-groups. Estimated vaccine efficacy (protection against carriage) was 66.87% (95% CI 50.49-82.26%), similar to previous estimates. 56 Ten-year projected vaccine impact (VT carriage reduction) among 0-9 years old was lower than observed in other settings, at 76.23% (CI 95% 68.02-81.96%), with sensitivity analyses 58 demonstrating this to be mainly driven by a high local force of infection.

60 **Conclusions:** We have identified both vaccine-related and host-related determinants of post-PCV13 62 pneumococcal VT transmission in Blantyre with vaccine impact determined by age-related characteristics of the local force of infection. These findings are likely to be generalisable to other 64 Sub-Saharan African countries in which PCV impact has been lower than desired, and have implications for the interpretation of post-PCV carriage studies and future vaccination programs.

64 Introduction

66 *Streptococcus pneumoniae* (pneumococcus) is a bacterial human pathogen commonly carried 68 asymptotically in the nasopharynx, which in a minority of carriers can cause severe disease such as pneumonia, meningitis or bacteraemia¹, posing a serious mortality risk, especially for young 70 children (<5 years of age), the elderly (>65 years of age) and the immunocompromised². Pneumococcal carriage is a necessary precursor of severe disease³ and transmission, such that reduction of carriage through active control is an important, universal public health goal.

72 Currently, pneumococcal conjugate vaccines (PCV) are the best available tool to reduce carriage 74 and disease both within risk groups and the general population. These vaccines have consisted of either 7, 10 or 13 polysaccharides conjugated to a carrier protein (PCV7, PCV10, PCV13, 76 respectively). All have been demonstrated to be highly protective against 7, 10 or 13 common pneumococcal serotypes associated with carriage and disease (also termed vaccine serotypes, VT). 78 A frequently observed consequence of PCV introduction is the increase in both carriage and disease of non-VT pneumococci (NVT), likely due to increased niche availability and reduction of competition between VT and NVT⁴⁻⁹.

80 PCV routine vaccination has been a common control strategy for over a decade in developed countries, with past experience showing that both pre- and post-PCV pneumococcal carriage can be highly variable within and between countries¹⁰⁻¹⁶. PCV vaccines have only recently been introduced

82 in Sub-Saharan African countries, such as Kenya^{17,18}, Malawi¹⁹, The Gambia²⁰ and South Africa²¹. In
84 November 2011, Malawi introduced the 13-valent pneumococcal conjugate vaccine (PCV13) as
86 part of the national extended program of immunization with a 3+0 schedule (at 6, 10 and 14 weeks
88 of age). With high routine coverage (~90%) and a small catch-up campaign of young children,
90 PCV13 was expected to quickly reduce carriage as previously reported in developed countries.
92 However, recently published data on nasopharyngeal carriage as measured in a cross-sectional
94 observational study in Blantyre (Southern Malawi), four to seven years after PCV13 introduction
96 (2015-2018), has shown that vaccine impact (VT carriage reduction) has been slower than expected
98 and heterogeneous across age-groups²². Epidemiological mathematical models have previously been
employed successfully to improve our understanding of pneumococcal dynamics^{5,9,23-27}, as well as
having contributed to explain, estimate and project PCV impact^{8,11,28}. The main advantage of models
is their cost-free potential to test hypotheses and gain a mechanistic, ecological and immunological
understanding of carriage and disease dynamics, estimating epidemiological parameters which are
difficult to otherwise quantify from raw epidemiological data. For example, models have
successfully yielded estimates of VT and non-VT pneumococci transmission potentials^{26,29-31},
pneumococcal competition factors^{8,9,23,28,32,33} and measures of vaccine-induced protection from
carriage at the individual level^{11,17,28,34,35}, none of which are readily observed or quantified in cross-
sectional observational studies.

100 In this study we use a Bayesian Markov chain Monte Carlo fitting approach and a dynamic model
102 to investigate the post-PCV13 pneumococcal VT carriage dynamics in Blantyre, Malawi. We find
104 that natural immunity and age-specific transmission potentials are necessary to reproduce observed
106 VT carriage. When compared to numerous literature reports from other regions, our estimated
108 vaccine efficacy (individual-level protection from carriage) was close to expected values, but
110 impact (population-level reduction of VT carriage) was lower both in the short- and long-term. We
show that vaccine impact was likely being offset by a high local force of infection compared to
other regions of the world. Our study offers key insights into the lower than expected PCV13
impact in Malawi and more generally on the heterogeneous nature of pre- and post-vaccination
pneumococcal VT carriage across age-groups and regions. These results can be translated to other
Sub-Saharan African countries in which PCV impact has been lower than desired.

Methods

112 **Prospective cross-sectional observational study**

114 An observational study using stratified random sampling was conducted to measure pneumococcal
116 nasopharyngeal carriage in Blantyre, Malawi²². Sampling was performed twice a year, between June
118 and August 2015 (survey 1), October 2015 and April 2016 (survey 2), May and October 2016
(survey 3), November 2016 and April 2017 (survey 4), May and October 2017 (survey 5);
November 2017 and June 2018 (survey 6), and June and December 2018 (survey 7). In this study,
120 we use the mid-point dates of the surveys for model fitting and presentation of results. A total of
7148 individuals were screened with nasopharyngeal swabs processed following WHO
recommendations³⁶. Isolates were serotyped by latex agglutination (ImmunoLex™ 7-10-13-valent
Pneumotest; Statens Serum Institute, Denmark). In this study, we use all the data from three age-
122 groups: 499 vaccinated children 2 years old, 2565 vaccinated children 3–7 years old and 1402

124 unvaccinated children 3–10 years old. For the first three surveys, data on vaccinated 2 years old
125 individuals was not collected. Observed VT carriage levels are presented in Figure 1d (and Table
126 S7). Further details on collection, processing and observations, have been previously described in
detail²².

Vaccine type transmission model

128 A deterministic, ordinary-differential equations (ODE) model (Figure 1a) was developed to fit VT
carriage levels as reported in the cross-sectional observational study in Blantyre (Figure 1d)²².
130 Fitting was implemented using a Bayesian Markov chain Monte Carlo (bMCMC) approach
developed and used by us in other modelling studies^{37–39}, including informative priors for duration
132 of carriage (Figure 1b, Table S1) and uninformative uniform priors for vaccine efficacy (individual-
level protection against carriage) and transmission potential. The methodology is summarised in
134 this section and further details such as equations, literature review on priors and expected parameter
values (Tables S1, S2, S5, S6) and complementary results can be found in Supplementary Text S1.

136

Pneumococcal infection dynamics and human demographics

138 As depicted in Figure 1a, the population was divided into seven non-overlapping age-groups: 0
(<1), 1, 2, 3-5, 6-7, 8-9, 10+ years old. Ageing was approximated by moving individuals along age-
140 groups with a rate ($a_{age-group}$) equal to the inverse of the time spent at each age class. The seven age-
groups were further divided into vaccinated ($S_{age-group}^v$, $C_{age-group}^v$) and unvaccinated ($S_{age-group}$, $C_{age-group}$)
142 susceptibles (S) and carriers (C). The population size was assumed to be constant, with total deaths
equal to births (details in Supplementary Text S1). Death rates were age-specific ($\mu_{age-group}$) and
144 relative to a generalized total life-span of 70 years.

146 **Natural immunity**

148 Pneumococcal colonization increases both humoral (anti-capsular serotype-specific and anti-protein
non-serotype-specific) and T-cell (anti-protein) immunity⁴⁰. Acquisition of this immunity correlates
150 with colonization in children and increases with age as colonization decreases. In our model (Figure
151 1a), all individuals were assumed to be born susceptible but can acquire infection (colonization) at
any age with a particular force of infection $\lambda_{age-group}$, becoming carriers ($C_{age-group}$) for an age-
152 specific period ($1/\gamma_{age-group}$), and returning to the susceptible state ($S_{age-group}$) after clearance. Hence,
the development of complete (sterile) immunity to the pneumococcus was not considered. We
154 nonetheless allowed for decreasing duration of carriage with age ($1/\gamma_{age-group}$) as a proxy for the
development of pneumococcal immunity with age. To quantify differences in age, we used carriage
156 duration data as reported by Hogberg and colleagues⁴¹ to define informative priors related to the
aggregated age-groups: 0-2 years ($1/\gamma_{0-2}$), 3-5 years ($1/\gamma_{3-5}$), 6-8 years ($1/\gamma_{6-8}$), and 8+ years ($1/\gamma_{8+}$) as
158 represented in Figure 1b (Table S1 for literature review).

160 **Vaccination, efficacy and impact**

162 For simplicity, routine vaccination was implemented at birth with coverage (ρ) at 92.5%²², and
163 catch-up (k) implemented as a one-off transfer of a proportion of individuals from the unvaccinated
164 susceptibles with 0 (<1) years of age (S_0) to the vaccinated susceptible class with the same age (S^v_0)
165 with coverage of 60%²². We assumed the vaccine to reduce the risk of infection (colonization) of
166 vaccinated individuals by a proportion ζ (between 0 and 1, with $\zeta=1$ equating to no risk). This
167 reduction in risk was herein defined and interpreted as the individual-level vaccine efficacy against
168 carriage ($VE = 100 \times \zeta$), and was modelled directly on the force of infection (λ) (Figure 1a, and
169 Table S2 for literature review). We measured vaccine impact across age-groups as the post-PCV13
170 percent reduction in population-level VT carriage compared to pre-vaccination levels.

170 **Force of infection**

172 We considered several transmission matrices (Supplementary Text S1), and compared the resulting
173 model fits using leave-one-out cross-validation (LOO) and the widely applicable information
174 criterion (WAIC) measures. The inhomogeneous transmission matrix presented in Figure 1c over-
175 performed the others and was used for the results presented in the main text. Its structure is based
176 on epidemiological studies conducted in American, European and African populations reporting
177 typical, strong, intrinsic variation in frequency, efficiency and environmental risk of transmission
178 between age-groups^{10,31,42-47}. In summary, the transmission matrix is generally populated with a
179 baseline coefficient β , and a different coefficient θ assigned to transmission occurring within and
180 between ages 0-5 years, and within 6-7 and 8-9 years of age independently. Further literature
181 support and results from the second best performing transmission matrix can be found in
182 Supplementary Text S1.

184 **Fitting to survey data**

186 The model's carriage outputs for vaccinated 2, vaccinated 3-5, unvaccinated 6-7 and unvaccinated
187 8-9 years of age, were fitted to observed levels in Blantyre's 1-7 surveys (Figure 1d, values in Table
188 S7), approximately four to seven years PCV13 introduction (2015-2018). A total of seven
189 parameters were fitted: vaccine efficacy against carriage (ζ , uninformative prior), coefficients of
190 transmission (β , θ , uninformative priors) and durations of carriage in ages 0-2, 3-5, 6-7, 8+ years (1/
191 γ_{0-2} , 1/ γ_{3-5} , 1/ γ_{6-8} , 1/ γ_{8+} , informative priors). The transmission model was initialized at time $t=0$ with a
192 proportion of 0.99 susceptibles and 0.01 infected, with numerical simulations run until an
193 equilibrium was reached. At equilibrium, vaccination was introduced and the first post-vaccine 15
194 years recorded. Levels of carriage in the model were calculated as the proportion of individuals
195 within an age-group that are carriers (i.e. $C/(S+C)$, expressions in Supplementary Text S1). The
196 model was run with parameters scaled per year. bMCMC chains were run for 5 million steps, with
burn-in of 20% (bMCMC details in see Supplementary Text S1).

198 **Results**

199 We used our deterministic transmission model and bMCMC approach to fit the observed post-
vaccination VT carriage data from Blantyre, Malawi (2015 - 2018). Based on this fit, we could

200 reconstruct age-specific carriage dynamics for the unobserved first four years (2011 – 2015), and
201 project VT carriage reduction into the future, to identify the mechanistic nature of the slow PCV13
202 impact on the vaccinated age-groups and strong herd-effects in the older unvaccinated age-groups.

204 **Model fit and posteriors**

205 VT carriage levels across age-groups reported from the surveys were closely reproduced by the
206 mean and 95% CI of the model using the bMCMC approach (Figure 2a). Our initial assumption of
207 natural immunity accumulating with age was generally respected in the bMCMC solution (Figure
208 2b); i.e. the estimated posterior distributions of the durations of carriage ($1/\gamma_{\text{age-group}}$) were adjusted
209 by the bMCMC by approximately -0.7, +0.64, +0.58 and -1.73 days for the age-groups 0-2, 3-5, 6-7
210 and 8+ years of age, respectively. The posterior distribution of vaccine efficacy (individual-level
211 protection against carriage) across ages was estimated to be 66.87% (95% CI 50.49-82.26). While
212 we used an uninformative prior (uniform, 0 to 1) in the bMCMC, this efficacy posterior was similar
213 to others recently estimated with different models and in multiple epidemiological settings (Figure
214 2c). We therefore argue that it serves as partial validation for our modelling framework. Finally, the
215 solutions for the transmission coefficients β and θ suggested that in order to reproduce the Blantyre
216 survey data, the risk of infection associated with contacts within and between younger age-groups
217 (0-5 years old) would have to be higher than that of the general population (i.e. $\theta >> \beta$).

218

Vaccine impact across age-groups

220 Using parameter samples from the bMCMC estimated posteriors, we simulated vaccine impact in
221 terms of VT carriage reduction across age-groups in the first 10 years post-vaccination (Figure 3).

222 After the first year, VT carriage reduction was estimated to be 42.38% (95% CI 37.23-46.01%) for
223 the 0 (<1) years old, followed by 29.25% (95% CI 26.4-31.4%) for the 1 years old, 17.45% (95%
224 CI 16.47-18.36%) for the 2 years old and 4.95% (95% CI 8.78-10.89%) for 3-5 years old (Figure
225 3a). With time, as carriage generally dropped and vaccinated individuals aged, the older groups
226 were estimated to benefit from increasingly similar reductions in carriage compared to the initially
227 vaccinated group. Since during the first year only the 0 (<1) years of age were vaccinated, the short-
228 term reductions in carriage of the other groups were due to indirect herd-effects alone.

229 At the target point of 10 years into the post-vaccination era, impact was estimated to be similar
230 across all age-groups, with VT carriage reduced by 76.9% (CI 95% 68.93-82.32%) for the 0 (<1)
231 years old, 75.72% (CI 95% 67.78-81.24%) for the 1 years old, 75.51% (CI 95% 67.55-81.05%) for
232 the 2 years old and 75.86% (CI 95% 68.29-80.97%) for 3-5 years old. We further projected vaccine
233 impact on aggregated age-groups 0-5 and 6-9 years of age, which showed equivalent reductions in
234 VT carriage (Figure 3b), with the larger aggregated age-group 0-9 years old having a total reduction
235 of 76.23% (CI 95% 68.02-81.96%) after 10 years.

236 We performed a literature review on observed reduction of VT carriage in time after the
237 introduction of PCV vaccines (Table S5) in numerous countries, and concluded that both the
238 observed carriage levels during the surveys and during the model's projection for the first 10 years
239 were high when compared to other countries. For instance, residual carriage of PCV13 types was

240 0.4% after 4 years of vaccination in England⁴⁸, 9.1% after 2 years of vaccination in Italy⁴⁹, and 7%
241 after 3 years of vaccination in Alaska, USA¹⁶. Similarly, for 0-5 year old individuals, PCV10 in
242 Kenya¹⁸ has reduced VT carriage by 73.92% in the first 5 years, while in Portugal⁵⁰, PCV7 has
243 reduced VT carriage by 78.91% in the same age-group and amount of time (more examples can be
244 found on Table S5).

Post-vaccination changes in force of infection

246 To try to understand responses to vaccination across age-groups, we further explored the post-
247 PCV13 force of infection (FOI) dynamics. The FOI is the overall rate by which a certain age-group
248 of susceptible individuals is infected, comprising the transmission rate (β or θ) weighted by the
249 number of infectious individuals within the same and other age-groups. Although we modelled six
250 independent age-groups under 10 years of age, only three unique FOIs are defined in the
251 transmission matrix for individuals under 9 years of age (0-5, 6-7 and 8-9 years of age, Figure 1c).
252 As determined by the posteriors of β and θ (Figure 2d), the pre-vaccination absolute FOI of the 0-5,
253 6-7 and 8-9 age-groups was different at PCV13 introduction, and with vaccine roll out the FOI of
254 each age-group decreased in time (Figure 4a). We also examined the FOI derivative with respect to
255 time as a measure of speed of FOI reduction (Figure 4b), and found that the time period of fastest
256 FOI reduction for the 0-5 years old was between vaccine introduction and 2015 (when no carriage
257 data was collected). This contrasted with the older age-groups (6-7 and 8-9), for which the period of
258 fastest FOI reduction was predicted to be just before or during the first three surveys. Thus,
259 although surveys 1 to 7 suggest a rather slow reduction of VT carriage for the younger age-groups
260 during the observational study, this seems to have been preceded by a period of high, short-term
261 impact on VT carriage for those age-groups (seen in the initial dynamics of Figures 3a and 3b).
262 Indeed, vaccine impact (reduction in VT carriage) at the time of the first survey was estimated to be
263 46.9% (95% CI 43.2-49.42) for the aggregated age-group 0-5 years old. At the same time, the
264 fastest reduction in FOI for the older age-groups was predicted by the model to take place just
265 before and during the first surveys, the time period in which survey data presents the largest
266 reductions in VT carriage for those age-groups (Figure 1d). Overall, projected FOI dynamics
267 suggest that PCV13 impact has been non-linear in time within age-groups, with predicted periods of
268 faster reductions in VT carriage being experienced by different ages in a sequential manner, from
269 younger to older individuals.

270

Sensitivity of vaccine impact based on transmission setting

272 The projected impacts of Figures 3 and 4 were based on the estimated transmission coefficients for
273 Blantyre (Figures 1b and 2d). To contextualize this particular transmission setting, we searched the
274 literature for pre-vaccination VT carriage levels in other countries (Table S6). The reported age-
275 groups were highly variable, and we therefore focused on the 0-5 years old group for which more
276 data points were available from a range of countries in North America, Africa, Europe and South-
277 east Asia (Figure 5a). Reported VT carriage in this age-group was highly variable both between and
278 within countries, with our estimation for Blantyre being on the higher end (61.58%, 95% CI 50.0-
279 70.9%).

280 We further searched the literature for post-vaccination VT carriage levels in other countries and
281 again focused on the age-group 0-5 years old for which more data points were available (Table S5,
282 points with whiskers in Figure 5b). The projected impact for Blantyre according to our model
283 (dashed line), was notably lower than observed for other countries. A Malawi data point reported in
284 the context of the Karonga District (Northern Malawi) had the closest impact to our projections in
285 Blantyre (Southern Malawi), 4 to 5 years after PCV13 introduction¹⁹.

286 Given that our posterior of vaccine efficacy (individual-level protection against carriage, Figure 2c)
287 was close to estimations from other regions of the world, we hypothesised that both the higher pre-
288 and post-PCV13 VT carriage levels in Blantyre were likely due to a higher local force of infection
289 compared to other regions. To demonstrate this, we simulated a range of alternative transmission
290 settings in Blantyre, by varying both the transmission coefficients (β and θ) between -70% and
291 +120% of their estimated posteriors (full exercise in Figure S3). This sensitivity exercise showed
292 that lowering local transmission by approximately -30% was sufficient for the model to
293 approximate short- and long-term vaccine impact observed in several other countries (Figure 5b).
294 Other age-groups, for which far less data points were available, presented similar patterns (Figure
295 S4).

296 **Discussion**

297 Using a dynamic model, we have reproduced observed changes in pneumococcal VT carriage
298 following the introduction of PCV13 in Blantyre, Malawi. Similar to other modelling frameworks
299 we have considered the accumulation of natural immunity with age and have also allowed for
300 heterogeneous transmission potentials within and between age-groups. Including these factors
301 allowed us to identify age-related characteristics of the local force of infection as the main
302 determinants of the high residual pneumococcal vaccine type carriage in Blantyre, seven years post-
303 PCV13 introduction.

304 A main motivation for developing our dynamic model was to explain the high residual VT carriage
305 levels seven years post-PCV13 introduction²². Studies from Kenya, The Gambia and South Africa
306 have reported similar trends, with VT carriage remaining higher than in industrialised countries at
307 similar post-vaccination time points. Compared to studies from other geographical regions, pre- and
308 post-vaccination VT carriage in Blantyre was at the upper end of reported values across many
309 countries (Figure 5 and Tables S5, S6). Given that our estimate of vaccine efficacy (individual-level
310 protection against carriage) was similar to reports from elsewhere (Figure 2c, Table S2), we tested
311 the hypothesis that the observed and projected lower vaccine impact was likely a result of a higher
312 force of infection in Blantyre compared to other regions. This force of infection was found to be
313 characterised by different transmission potentials within and between age-groups, and particularly
314 dominated by individuals younger than 5 years. Reflecting a variety of approaches and assumptions
315 that can be found in other models^{8,11,28}, our framework is not able to discern if this assortative
316 relationship with age is due to age-specific contact type patterns or susceptibility to colonization.
317 Nonetheless, our results strongly argue for the need of more research characterising local contact,
318 risk and transmission-route profiles (e.g. ⁴²), if we are to understand the myriad of reported PCV
319 impacts across different demographic, social and epidemiological settings.

320 There were also the observations of vaccine impact (reduction in VT carriage) in unvaccinated age-
321 groups, and a particularly slow impact in younger vaccinated age-groups during the surveys (Figure
322 1d). The dynamic model helped explain these age-related responses, by showing that age-groups
323 have experienced periods of higher vaccine impact at different time points, sequentially, from
324 younger to older groups. A major implication is that reduction in VT carriage in vaccinated younger
325 age-groups has been fastest between PCV13 introduction and 2015, when no carriage data was
326 collected in Blantyre, but consistent with data collected in rural northern Malawi¹⁹. Thus, similarly
327 to the conclusions of another modelling study²⁸, our results advocate for the essential role of
328 dynamic models to understand post-PCV13 VT carriage, by critically accounting for local non-
329 linear effects of pneumococcal transmission and vaccination which may have significant
330 implications for data interpretation.

331 Critical for low and middle income countries, as well as global initiatives such as Gavi, is that the
332 impact of PCVs on pneumococcal VT carriage needs to be further improved if we are to maximize
333 disease reduction. For high burden countries like Malawi, in which post-PCV VT carriage data
334 suggests that local epidemiological factors may dictate lower vaccine impact than elsewhere,
335 region-specific improved vaccination schedules^{19,22} and catch-up campaigns²⁸ could help speed-up
336 VT carriage reduction and maximise cost-effectiveness. For this to be possible, we need to better
337 understand local transmission profiles across ages, which are likely dictated by demographic and
338 socio-economic factors, and strongly determine short- and long-term PCV impact.

Limitations

340 Data suggest that immune responses to PCV vaccines wane over time^{22,34}. In a meta-analysis study,
341 PCV7 efficacy was estimated at 62% (CI 95% 52-72%) at four months post-vaccination, decreasing
342 to 57% (CI 95% 50-65%) at six months, but remaining 42% (CI 95% 19-54%) at five years post-
343 vaccination³⁴. Models implicitly parametrising for duration of vaccine-induced protection (dVP)
344 have typically followed a prior with minimum mean duration of six years^{8,11,28,34}, but in one study
345 dVP was estimated as 8.3 years (95% CI 5 – 20)⁸. Our framework does not explicitly include dVP,
346 and this should be a line of future modelling research. Due to the time ranges studied for Blantyre
347 (data were collected up to seven years post-PCV13 introduction and projections made only up to the
348 first ten years), we argue that our results should be robust and only weakly influenced by not
349 considering dVP. In light of the possibility that dVP is shorter than previously reported²², our
350 projections of vaccine impact should be seen as a best-case scenario; i.e. real long-term vaccine
351 impact in Blantyre would likely be lower than projected by our model. Our framework also does not
352 include niche competition between VT and non-VT pneumococci^{11,28,34}. It is difficult to assert the
353 impact of such competition in our main results, but it is unlikely that our conclusions would be
354 significantly affected, since they are mostly based on factors which have not been reported to be
355 associated with type competition directly (e.g. age-specific transmission).

Conclusion

356 In Blantyre, vaccine efficacy (individual-level protection against carriage) across ages and time was
357 estimated at 66.87% (95% CI 50.49-82.26%), similar to reports from other countries. However,
358 local transmission potential in Blantyre is likely to be higher than in other countries and also

360 heterogeneous among age-groups, with a particular contribution from younger children. While
361 PCV13 is achieving positive outcomes in Blantyre^{19,51}, a local higher and age-dependent force of
362 infection is dictating a lower long-term vaccine impact (population-level carriage reduction) than
363 reported elsewhere. Finally, the combination of age-related transmission heterogeneities and
364 routinely vaccinating infants has led to non-linear responses in terms of vaccine impact across ages
365 and time, with general implications on post-vaccination VT carriage data interpretation. Together,
366 these findings suggest that in regions with lower than desired PCV impact on VT carriage,
367 alternative vaccine schedules and catch-up campaigns targetting children <5 years of age should be
368 further evaluated.

Acknowledgements

370 We would like to thank Ellen Heinsbroek for key literature references used in this manuscript, and
371 Stefan Flasche for useful information regarding raw data of published studies. We thank the
372 individuals who participated in this study and the local schools and authorities for their support. We
373 are grateful to the study field teams (supported by Farouck Bonomali and Roseline Nyirenda) and
374 the study laboratory team. We are grateful to the MLW laboratory management team (led by
375 Brigitte Denis) and the MLW data management team (led by Clemens Masesa). RSH, NF and TS
376 are supported by the National Institute for Health Research (NIHR) Global Health Research Unit on
377 Mucosal Pathogens using UK aid from the UK Government. The views expressed in this
378 publication are those of the author(s) and not necessarily those of the NIHR or the Department of
379 Health and Social Care.

380 Funding

381 Bill & Melinda Gates Foundation, Wellcome Trust UK, Medical Research Council, European
382 Research Council, National Institute for Health Research.

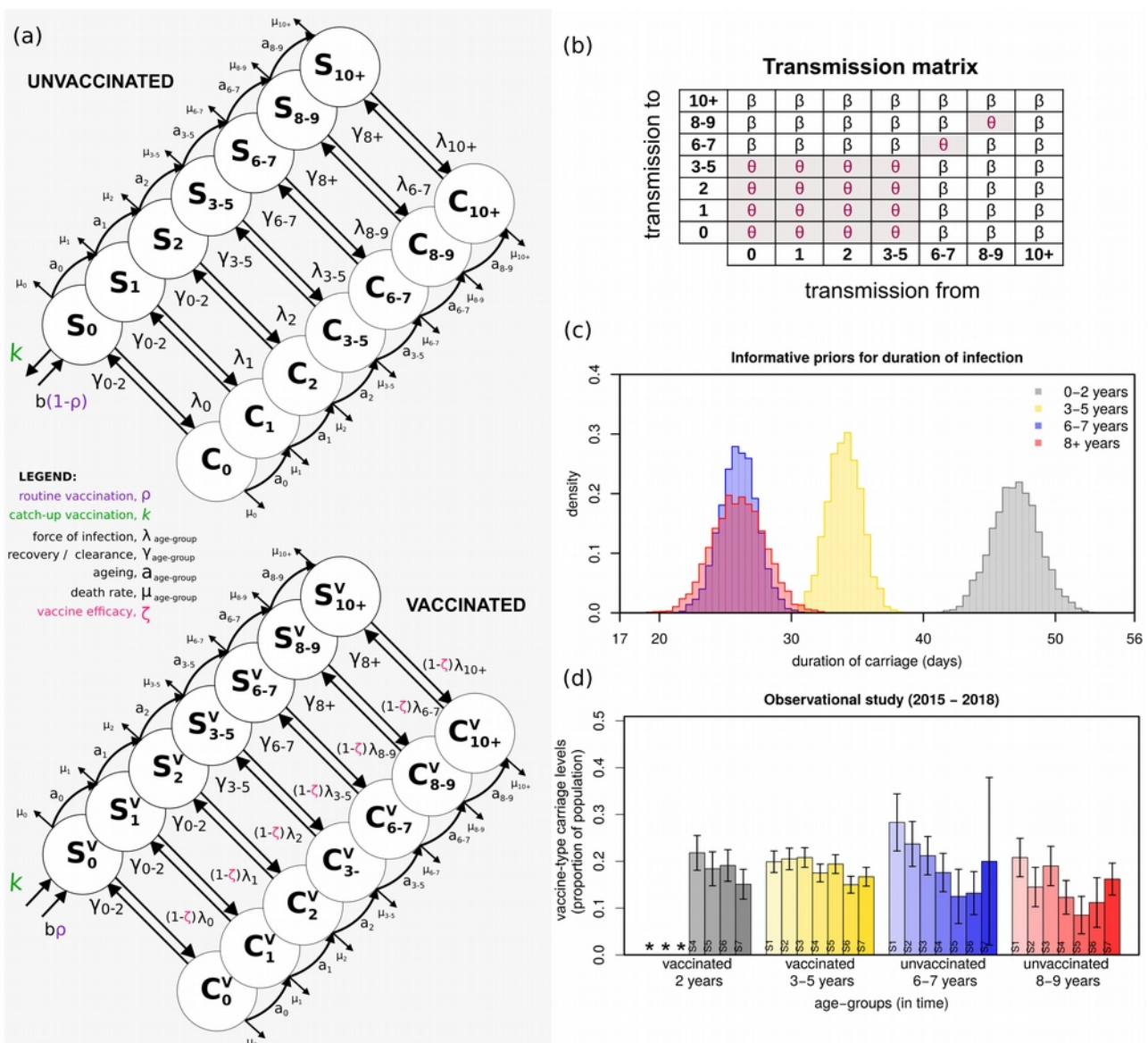
Contributions

383 JL, UO, TDS designed the modelling study. JL and UO designed the model. JL implemented the
384 model and the fitting approach. JL, UO analysed and interpreted model output. JL and UO searched
385 and curated the literature data. TDS supervised, while AG, NBZ, DE, AWK, TSM, AAM, CM and
386 MB collected and curated the Malawi observational data. SG, NF and RSH supervised both the
387 modelling and observational sides of the study. JL wrote the first draft of the manuscript which all
388 authors revised. JL, UO and TDS revised other iterations of the manuscript. All authors revised the
389 last version of the manuscript.

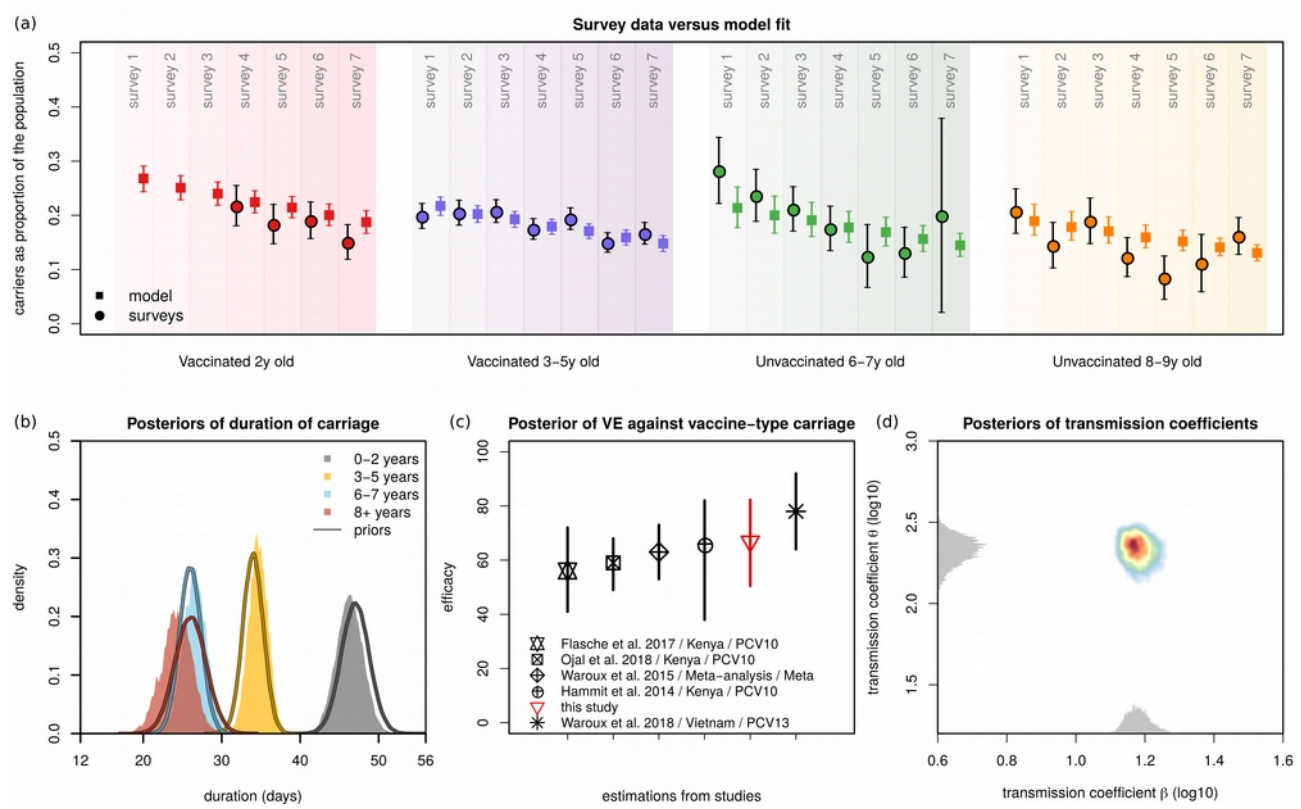
Declaration of interests

390 No other competing interests were reported by authors.

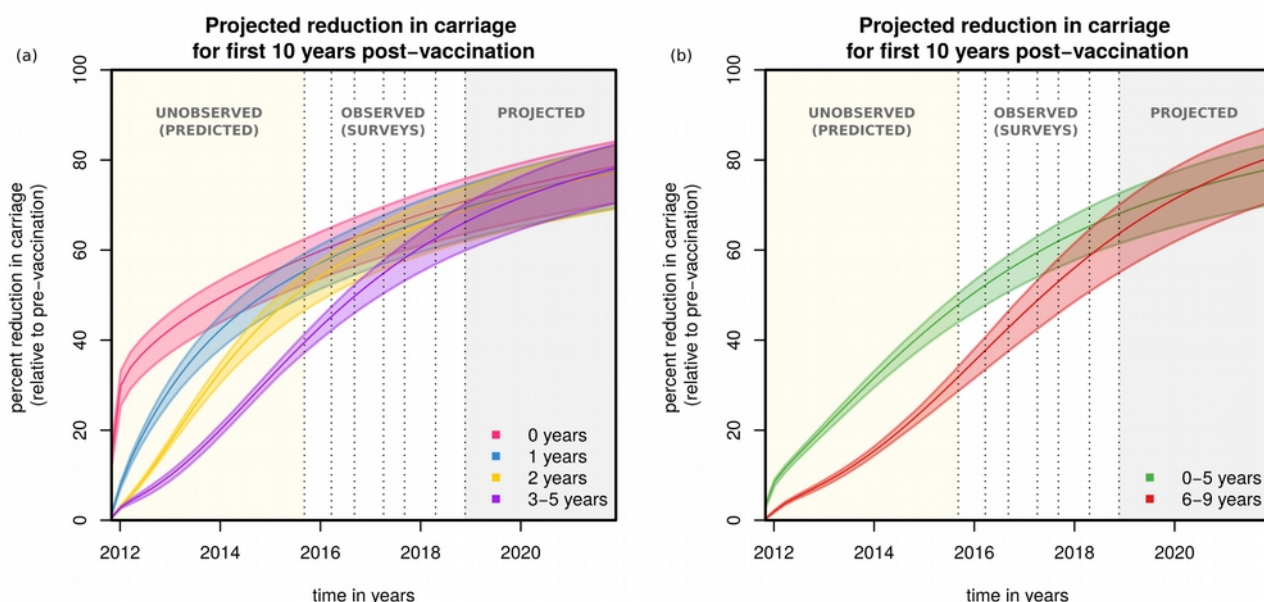
394 **Figures**



396 **Figure 1: Survey data and model framework, priors and transmission matrix.** (a) Seven age-
 397 groups were modelled: 0, 1, 2, 3-5, 6-7, 8-9, 10+ years of age (circles), each divided into
 398 unvaccinated (top) and vaccinated (bottom). Labels $a_{age\text{-}group}$ mark ageing rates per age class; $\mu_{age\text{-}group}$
 399 mark age-specific death rates; b marks births, at which point a proportion (ρ) are vaccinated
 400 (purple); ζ marks vaccine-induced protection, expressed as reduction in susceptibility to infection of
 401 vaccinated individuals (magenta); $\lambda_{age\text{-}group}$ mark age-specific forces of infection; $\gamma_{age\text{-}group}$ mark age-
 402 specific rates of clearance from infection; k marks catch-up vaccination (green). (b) The
 403 transmission matrix used, with coefficients β and θ , where θ is the specific coefficient for
 404 transmission within and between particular age-groups. β and θ are estimated when fitting the
 405 survey data. (c) The informative priors used in the fitting exercise for mean (standard deviation)
 406 infectious periods (days) of 47 (1.8) for 0-2 years old; 34 (1.3) for 3-5 years old; 26 (1.4) for 6-8
 407 years old; 26 (2.0) for 8+ years old (taken from [1]). The posterior values of these periods ($1/\gamma_{0-2}$, $1/\gamma_{3-5}$,
 408 $1/\gamma_{6-8}$, $1/\gamma_{8+}$) are estimated when fitting the survey data. (d) Mean and standard error for
 409 carriage as reported in the observational study data (surveys) per age-group (Table S7). S1 to S7
 410 highlight the surveys 1 to 7. The * mark data that was not collected.

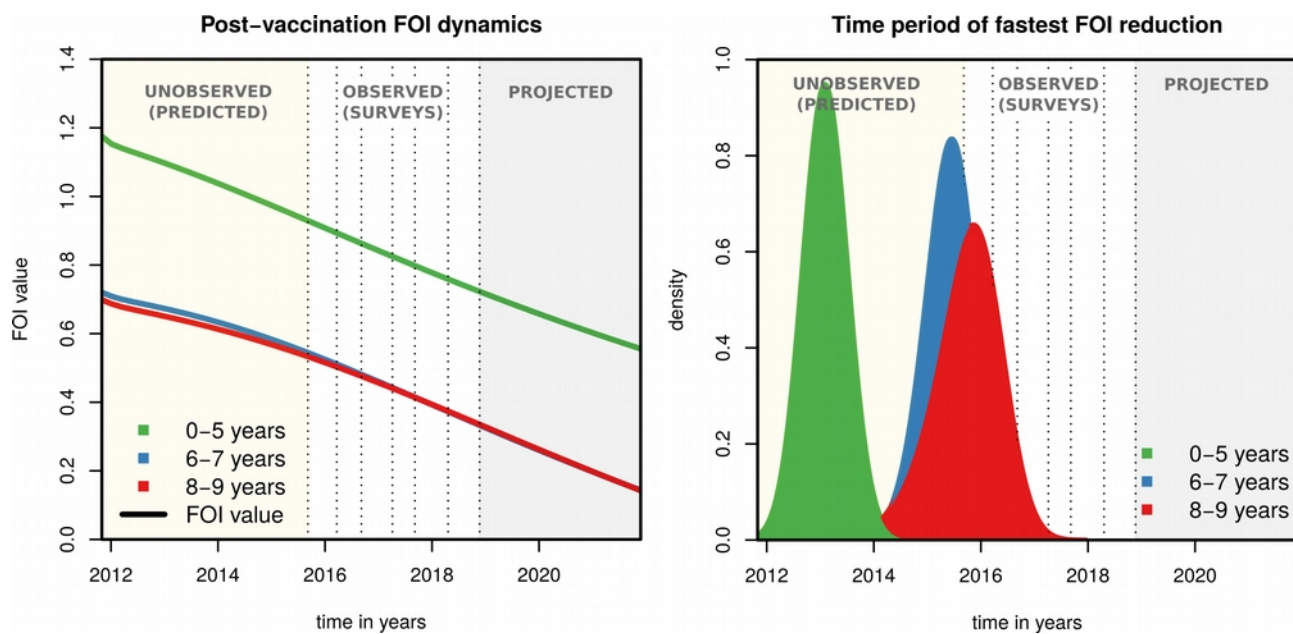


412 **Figure 2: Model fit and estimated posteriors.** (a) Model fit to carriage data from the
414 observational study for different age-groups: vaccinated 2 years old (red), vaccinated 3-5 years old
416 (purple), unvaccinated 6-7 years old (green) and unvaccinated 8-9 years old (orange). The survey
418 data is represented by full circles, the model output by full squares (data in Figure 1d, Table S7). (b)
420 Priors (lines) and estimated posterior distributions (shaded) of duration of carriage per age-group.
422 (c) Estimated mean and 95% CI of posterior of vaccine efficacy against vaccine-type carriage (red)
424 in the context of estimates from other studies (in legend, Table S2). (d) The estimated posterior
distributions of the transmission coefficients β and θ are shown in two dimensions (coloured area).
The estimated actual distribution for β is in the x-axis and θ in the y-axis (visualised in grey). Note
that, for visualisation purposes, the axes are \log_{10} -transformed and the grey distributions' height has
no scale (height is not quantified). (a,b,c,d) Solutions presented are obtained from sampling
100,000 parameter values from posteriors and simulating the dynamic model.



426 **Figure 3: Projections of post-vaccination vaccine-type carriage reduction.** (a) Projected
427 reduction in carriage relative to the pre-vaccination era for age-groups 0 years (magenta), 1 year
428 (blue), 2 years (yellow) and 3-5 years (purple) old. (b) Projected reduction in carriage relative to the
429 pre-vaccination era for aggregated age-groups 0-5 years (green) and 6-9 years (red) old (with
430 corresponding 95% CIs). (a,b) Solutions presented are obtained from sampling 100,000 parameter
431 values from posteriors and simulating the dynamic model. The shaded areas are yellow for the post-
432 vaccination period with no carriage data, white for the post-vaccination period with data, and grey
433 for the post-vaccination projected period up to 10 years. Dotted vertical lines mark survey dates.
434 The x-axis origin marks PCV13 introduction.

436



438 **Figure 4: Projections of post-vaccination changes in the force of infection. (a)** The post-
440 vaccination force of infection (FOI) of different age groups (0-5 years in green, 6-7 in blue and 8-9 in
442 red) as calculated for each of 100,000 simulations using parameter samples from posteriors. **(b)** For
444 each FOI of each age-group and each 100,000 simulations using parameter samples from posteriors,
446 the time point of minimum derivative was calculated, resulting in one distribution per age-group
448 (coloured curves, 0-5 years in green, 6-7 in blue, 8-9 in red). This time point is as a proxy for the
period of fastest FOI reduction. The shaded areas are yellow for the post-vaccination period with no
carriage data, white for the post-vaccination period with data, and grey for the post-vaccination
projected period up to 10 years. Dotted vertical lines mark survey dates. The x-axis origin marks
PCV13 introduction.

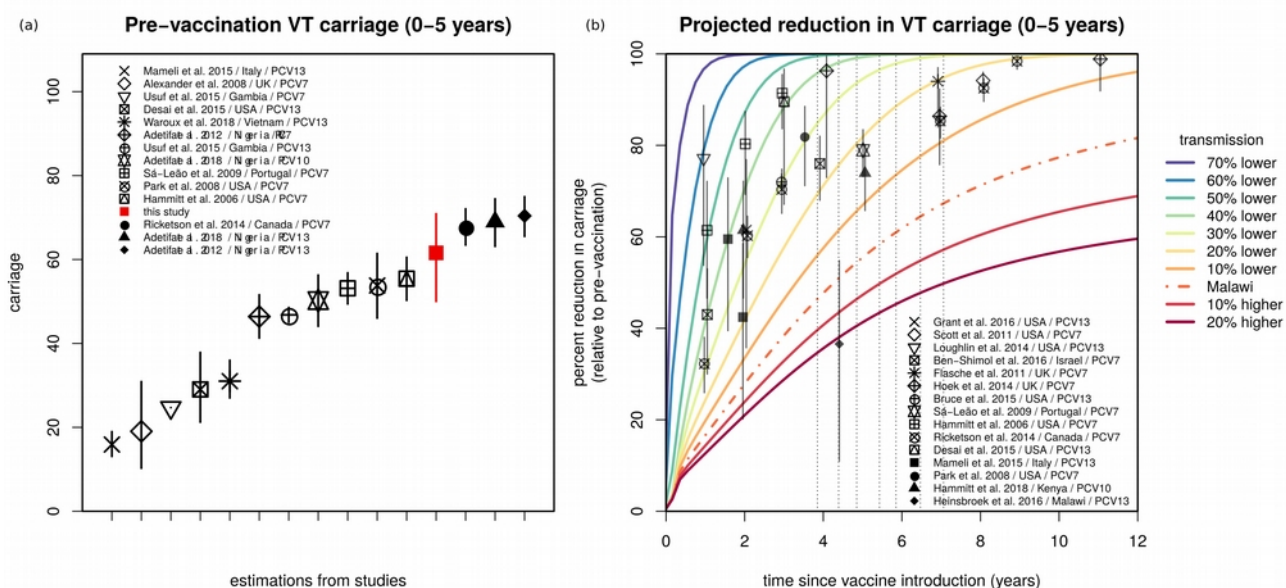


Figure 5: Estimated vaccine-type carriage and sensitivity of projections to baseline transmission in the context of other studies. (a) Estimated pre-vaccination vaccine-type carriage (and 95% CI) for the age-group 0-5 years of age (red) in the context of carriage levels reported in other studies (in legend, Table S6). **(b)** The baseline transmission coefficient (β) is varied by considering the 70%, 60%, 50%, 40%, 30%, 20%, and 10% lower, and 10%, 20% higher transmission than the estimated for Blantyre (Malawi, β_{Malawi}) when fitting the observational study (e.g. 10% lower is $0.9 * \beta_{\text{Malawi}}$). The impact projections for the age-group 0-5 years old using the β estimated for Blantyre (Malawi) are presented by the dashed line (as in Figure 3b). For visual purposes only the means are shown, obtained from simulations sampling 100,000 parameter values from posteriors. The symbols and whiskers are measures of reported impact (carriage reduction) and 95% CIs for several published studies (in legend, Table S5). The grey arrows mark the year of PCV13 introduction and the years of the four surveys.

References

464 1 Brown J, Hammerschmidt S, Orihuela C, editors. *Streptococcus Pneumoniae: Molecular*
466 *Mechanisms of Host-Pathogen Interactions*, 1st edn. Elsevier, 2015 DOI:10.1016/C2012-0-
00722-3.

468 2 Levine OS, O'Brien KL, Knoll M, *et al*. Pneumococcal vaccination in developing countries. *Lancet* 2006; **367**: 1880–2.

470 3 Simell B, Auranen K, Käyhty H, Goldblatt D, Dagan R, O'Brien KL. The fundamental link
472 between pneumococcal carriage and disease. *Expert Rev Vaccines* 2012; **11**: 841–55.

474 4 Weinberger DM, Malley R, Lipsitch M. Serotype replacement in disease after pneumococcal
476 vaccination. *Lancet* 2011; **378**: 1962–73.

478 5 Watkins ER, Penman BS, Lourenço J, *et al*. Vaccination Drives Changes in Metabolic and
480 Virulence Profiles of *Streptococcus pneumoniae*. *PLoS Pathog* 2015; **11**: e1005034.

482 6 Lourenço J, Wikramaratna PSPS, Gupta S. MANTIS: an R package that simulates multilocus
484 models of pathogen evolution. *BMC Bioinformatics* 2015; **16**: 176.

486 7 Ashby B, Watkins E, Lourenço J, Gupta S, Foster KR. Competing species leave many
488 potential niches unfilled. *Nat Ecol Evol* 2017; **1**. DOI:10.1038/s41559-017-0295-3.

490 8 Melegaro A, Choi YH, George R, Edmunds WJ, Miller E, Gay NJ. Dynamic models of
492 pneumococcal carriage and the impact of the Heptavalent Pneumococcal Conjugate Vaccine
on invasive pneumococcal disease. *BMC Infect Dis* 2010; **10**: 90.

494 9 Bottomley C, Roca A, Hill PC, Greenwood B, Isham V. A mathematical model of serotype
496 replacement in pneumococcal carriage following vaccination. *J R Soc Interface* 2013; **10**:
20130786–20130786.

498 10 Adetifa IMO, Antonio M, Okoromah CAN, *et al*. Pre-vaccination nasopharyngeal
500 pneumococcal carriage in a Nigerian population: Epidemiology and population biology.
502 *PLoS One* 2012; **7**. DOI:10.1371/journal.pone.0030548.

504 11 Le Polain de Waroux O, Edmunds WJ, Takahashi K, *et al*. Predicting the impact of
506 pneumococcal conjugate vaccine programme options in Vietnam. *Hum Vaccin Immunother*
508 2018; **0**: 1–21.

510 12 Cohen R, Levy C, Bonnet E, *et al*. Dynamic of pneumococcal nasopharyngeal carriage in
512 children with acute otitis media following PCV7 introduction in France. *Vaccine* 2010; **28**:
514 6114–21.

516 13 Collins DA, Hoskins A, Snelling T, *et al*. Predictors of pneumococcal carriage and the effect
518 of the 13-valent pneumococcal conjugate vaccination in the Western Australian Aboriginal
520 population. *Pneumonia* 2017; **9**: 14.

14 14 Spijkerman J, van Gils EJM, Veenhoven RH, *et al.* Carriage of *Streptococcus pneumoniae* 3
498 Years after Start of Vaccination Program, the Netherlands. *Emerg Infect Dis* 2011; **17**: 584–
91.

500 15 Desai AP, Sharma D, Crispell EK, *et al.* Decline in pneumococcal nasopharyngeal carriage of
502 vaccine serotypes after the introduction of the 13-valent pneumococcal conjugate vaccine in
children in Atlanta, Georgia. *Pediatr Infect Dis J* 2015; **34**: 1168–74.

504 16 Bruce MG, Singleton R, Bulkow L, *et al.* Impact of the 13-valent pneumococcal conjugate
506 vaccine (pcv13) on invasive pneumococcal disease and carriage in Alaska. *Vaccine* 2015; **33**:
4813–9.

508 17 Hammitt LL, Akech DO, Morpeth SC, *et al.* Population effect of 10-valent pneumococcal
510 conjugate vaccine on nasopharyngeal carriage of *Streptococcus pneumoniae* and non-
512 typeable *Haemophilus influenzae* in Kilifi, Kenya: Findings from cross-sectional carriage
studies. *Lancet Glob Heal* 2014; **2**: e397–405.

514 18 Hammitt LL, Etyang AO, Morpeth SC, *et al.* Effect of ten-valent pneumococcal conjugate
516 vaccine on invasive pneumococcal disease and nasopharyngeal carriage in Kenya: a
518 longitudinal surveillance study. *Lancet* 2019; **393**: 2146–54.

520 19 Heinsbroek E, Tafatatha T, Phiri A, *et al.* Pneumococcal carriage in households in Karonga
522 District, Malawi, before and after introduction of 13-valent pneumococcal conjugate
524 vaccination. *Vaccine* 2018. DOI:10.1016/j.vaccine.2018.10.021.

526 20 Roca A, Bojang A, Bottomley C, *et al.* Effect on nasopharyngeal pneumococcal carriage of
528 replacing PCV7 with PCV13 in the Expanded Programme of Immunization in The Gambia.
Vaccine 2015; **33**: 7144–51.

530 21 Nunes MC, Jones SA, Groome MJ, *et al.* Acquisition of *Streptococcus pneumoniae* in South
African children vaccinated with 7-valent pneumococcal conjugate vaccine at 6, 14 and 40
weeks of age. *Vaccine* 2015; **33**: 628–34.

532 22 Swarthout TD, Fronterre C, Lourenço J, *et al.* High residual prevalence of vaccine serotype
534 *Streptococcus pneumoniae* carriage 4 to 6 years after introduction of 13-valent pneumococcal
536 conjugate vaccine in Malawi: a prospective serial cross-sectional study. *bioRxiv* 2018;
published online Jan 1. <http://biorxiv.org/content/early/2018/10/26/445999.abstract>.

538 23 Obolski U, Lourenço J, Thompson C, Thompson R, Gori A, Gupta S. Vaccination can drive
an increase in frequencies of antibiotic resistance among nonvaccine serotypes of
540 *Streptococcus pneumoniae*. *Proc Natl Acad Sci* 2018; **115**: 3102–7.

542 24 McCormick AW, Whitney CG, Farley MM, *et al.* Geographic diversity and temporal trends
544 of antimicrobial resistance in *Streptococcus pneumoniae* in the United States. *Nat Med* 2003;
546 **9**: 424–30.

532 25 Lehtinen S, Blanquart F, Croucher NJ, Turner P, Lipsitch M, Fraser C. Evolution of antibiotic
534 resistance is linked to any genetic mechanism affecting bacterial duration of carriage. *Proc
Natl Acad Sci* 2017; **114**: 1075–80.

536 26 Huang SS, Finkelstein JA, Lipsitch M. Modeling Community- and Individual-Level Effects
of Child-Care Center Attendance on Pneumococcal Carriage. *Clin Infect Dis* 2005; **40**: 1215–
22.

538 27 Van Effelterre T, Moore MR, Fierens F, *et al.* A dynamic model of pneumococcal infection in
540 the United States: Implications for prevention through vaccination. *Vaccine* 2010; **28**: 3650–
60.

542 28 Flasche S, Ojal J, Le Polain de Waroux O, *et al.* Assessing the efficiency of catch-up
campaigns for the introduction of pneumococcal conjugate vaccine: A modelling study based
544 on data from PCV10 introduction in Kilifi, Kenya. *BMC Med* 2017; **15**: 1–10.

546 29 Melegaro A, Choi Y, Pebody R, Gay N. Pneumococcal carriage in United Kingdom families:
Estimating serotype-specific transmission parameters from longitudinal data. *Am J
Epidemiol* 2007; **166**: 228–35.

548 30 Melegaro A, Gay NJ, Medley GF. Estimating the transmission parameters of pneumococcal
carriage in households. *Epidemiol Infect* 2004; **132**: 433–41.

550 31 Nurhonen M, Cheng AC, Auranen K. Pneumococcal Transmission and Disease In Silico: A
552 Microsimulation Model of the Indirect Effects of Vaccination. *PLoS One* 2013; **8**.
DOI:10.1371/journal.pone.0056079.

554 32 Auranen K, Mehtälä J, Tanskanen A, S. Kaltoft M. Between-strain competition in acquisition
and clearance of pneumococcal carriage epidemiologic evidence from a longitudinal study of
556 day-care children. *Am J Epidemiol* 2010; **171**: 169–76.

558 33 Erästö P, Hoti F, Granat SM, Mia Z, Mäkelä PH, Auranen K. Modelling multi-type
560 transmission of pneumococcal carriage in Bangladeshi families. *Epidemiol Infect* 2010; **138**:
861–72.

562 34 Le Polain De Waroux O, Flasche S, Prieto-Merino D, Goldblatt D, Edmunds WJ. The
564 efficacy and duration of protection of pneumococcal conjugate vaccines against
nasopharyngeal carriage: A meta-regression model. *Pediatr Infect Dis J* 2015; **34**: 858–64.

566 35 Ojal J, Griffiths U, Hammitt LL, *et al.* The merits of sustaining pneumococcal vaccination
568 after transitioning from Gavi support - a modelling and cost-effectiveness study for Kenya.
bioRxiv 2018; published online Jan 1.
<http://biorxiv.org/content/early/2018/07/18/369603.abstract>.

566 36 Satzke C, Turner P, Virolainen-Julkunen A, *et al.* Standard method for detecting upper
568 respiratory carriage of *Streptococcus pneumoniae*: Updated recommendations from the
World Health Organization Pneumococcal Carriage Working Group. *Vaccine* 2013; **32**: 165–
79.

37 Lourenço J, de Lima MM, Faria NR, *et al.* Epidemiological and ecological determinants of
570 Zika virus transmission in an urban setting. *eLife* 2017; **6**. DOI:10.7554/eLife.29820.

38 Faria NR, da Costa AC, Lourenço J, *et al.* Genomic and epidemiological characterisation of a
572 dengue virus outbreak among blood donors in Brazil. *Sci Rep* 2017; **7**: 15216.

39 McNaughton AL, Lourenço J, Hattingh L, *et al.* HBV vaccination and PMTCT as elimination
574 tools in the presence of HIV: Insights from a clinical cohort and dynamic model. *BMC Med*
2019; **17**: 1–15.

576 40 Weiser JN, Ferreira DM, Paton JC. *Streptococcus pneumoniae*: Transmission, colonization
and invasion. *Nat Rev Microbiol* 2018; **16**: 355–67.

578 41 Hogberg L, Geli P, Ringberg H, Melander E, Lipsitch M, Ekdahl K. Age- and Serogroup-
580 Related Differences in Observed Durations of Nasopharyngeal Carriage of Penicillin-
Resistant Pneumococci. *J Clin Microbiol* 2007; **45**: 948–52.

582 42 le Polain de Waroux O, Cohuet S, Ndazima D, *et al.* Characteristics of human encounters and
social mixing patterns relevant to infectious diseases spread by close contact: A survey in
Southwest Uganda. *BMC Infect Dis* 2018; **18**: 1–12.

584 43 Althouse BM, Hammitt LL, Grant L, *et al.* Identifying transmission routes of *Streptococcus*
586 *pneumoniae* and sources of acquisitions in high transmission communities. *Epidemiol Infect*
2017; **145**: 2750–8.

588 44 Ojal J, Flasche S, Hammitt LL, *et al.* Sustained reduction in vaccine-type invasive
pneumococcal disease despite waning effects of a catch-up campaign in Kilifi, Kenya: A
mathematical model based on pre-vaccination data. *Vaccine* 2017; **35**: 4561–8.

590 45 Camilli R, Daprai L, Cavrini F, *et al.* Pneumococcal Carriage in Young Children One Year
after Introduction of the 13-Valent Conjugate Vaccine in Italy. *PLoS One* 2013; **8**: 1–10.

592 46 Mossong J, Hens N, Jit M, *et al.* Social contacts and mixing patterns relevant to the spread of
infectious diseases. *PLoS Med* 2008; **5**: 0381–91.

594 47 Kiti MC, Kinyanjui TM, Koech DC, Munywoki PK, Medley GF, Nokes DJ. Quantifying age-
596 related rates of social contact using diaries in a rural coastal population of Kenya. *PLoS One*
2014; **9**. DOI:10.1371/journal.pone.0104786.

598 48 Van Hoek AJ, Sheppard CL, Andrews NJ, *et al.* Pneumococcal carriage in children and adults
two years after introduction of the thirteen valent pneumococcal conjugate vaccine in
England. *Vaccine* 2014; **32**: 4349–55.

600 49 Mameli C, Fabiano V, Daprai L, *et al.* A longitudinal study of *streptococcus pneumoniae*
602 carriage in healthy children in the 13-valent pneumococcal conjugate vaccine era. *Hum
Vaccin Immunother* 2015; **11**: 811–7.

604 50 Sá-Leão R, Nunes S, Brito-Avô A, *et al.* Changes in pneumococcal serotypes and
antibiotypes carried by vaccinated and unvaccinated day-care centre attendees in Portugal, a

country with widespread use of the seven-valent pneumococcal conjugate vaccine. *Clin Microbiol Infect* 2009; **15**: 1002–7.

51 McCollum ED, Nambiar B, Deula R, *et al.* Impact of the 13-valent pneumococcal conjugate vaccine on clinical and hypoxemic childhood pneumonia over three years in central Malawi: An observational study. *PLoS One* 2017; **12**: 1–17.

610